Applied Earth Science

Transactions of the Institutions of Mining and Metallurgy

ISSN: (Print) (Online) Journal homepage: https://www.tandfonline.com/loi/yaes21

Predicting grade-tonnage characteristics of undiscovered mineralisation: application of the USGS Three-part Undiscovered Mineral Resource Assessment to the Sandstone Greenstone Belt of the Yilgarn Block, Western Australia

Rhys S. Davies , Richard Schodde , John P. Sykes , David I. Groves , Allan Trench & Michael Dentith

To cite this article: Rhys S. Davies , Richard Schodde , John P. Sykes , David I. Groves , Allan Trench & Michael Dentith (2020): Predicting grade-tonnage characteristics of undiscovered mineralisation: application of the USGS Three-part Undiscovered Mineral Resource Assessment to the Sandstone Greenstone Belt of the Yilgarn Block, Western Australia, Applied Earth Science, DOI: 10.1080/25726838.2020.1783740

To link to this article: https://doi.org/10.1080/25726838.2020.1783740

Published online: 23 Jun 2020.

APPLIED EARTH SCIENCE (TRANS. INST. MIN. METALL. B)
https://doi.org/10.1080/25726838.2020.1783740

The Institute of Materials, Minerals and Mining
AusIMM THE MINERALS INSTITUTE
Taylor & Francis
Taylor & Francis Group

Predicting grade-tonnage characteristics of undiscovered mineralisation: application of the USGS Three-part Undiscovered Mineral Resource Assessment to the Sandstone Greenstone Belt of the Yilgarn Block, Western Australia

Rhys S. Davies [a], Richard Schodde[a,b], John P. Sykes [a,b,c,d], David I. Groves[a,e], Allan Trench[a,d] and Michael Dentith[f]

[a]Centre for Exploration Targeting, School of Earth Sciences, The University of Western Australia, Crawley, Australia; [b]MinEx Consulting, South Yarra, Australia; [c]Greenfields Research Ltd, Harrogate, North Yorkshire, UK; [d]Business School, The University of Western Australia, Crawley, Australia; [e]Orebusters Pty Ltd, Gwelup, Australia; [f]School of Earth Sciences, The University of Western Australia, Crawley, Australia

ABSTRACT

The United States Geological Survey (USGS) Three-part Undiscovered Mineral Resource Assessment provides a framework for estimating undiscovered mineral endowment. Previous studies that applied the Three-part Assessment to estimate the undiscovered orogenic gold endowment of the Sandstone Greenstone Belt, Western Australia, have relied upon dated or expert-derived grade-tonnage models. Here, several assessments are conducted using local grade-tonnage models, comprising known orogenic gold deposits within the entire Yilgarn Block and several individual terranes with contrasting lithosphere- to terrane-scale characteristics. These models are generated through comprehensive review of historical exploration, resource and production data. Based on these models, the Sandstone Greenstone Belt is estimated to contain significant undiscovered gold mineralisation, with a median total endowment of between 166 and 298 t gold, and mean of 167–319 t gold. Although these updated grade-tonnage models provide an approximately 80 per cent variation in predicted gold endowment, it is still evident that the belt remains an under-explored region within the Yilgarn Block, Western Australia.

ARTICLE HISTORY
Received 11 March 2020
Revised 9 June 2020
Accepted 9 June 2020

KEYWORDS
Sandstone Greenstone Belt; Yilgarn Block; orogenic gold; USGS Three-part Undiscovered Mineral Resource Assessment

Introduction

Defining regions likely to contain significant undiscovered mineral endowment, and thus the potential cost–benefit of exploration activities, represents a key stage in the exploration decision-making process (Woodall 1994; Hronsky and Groves 2008; Kreuzer et al. 2008; Davies et al. 2020a). By generating quantitative estimates for undiscovered mineral endowment, the United States Geological Survey (USGS) Three-part Undiscovered Mineral Resource Assessment (Figure 1) provides a range of likely values for contained mineral resources.

During application of the Three-part Assessment, a permissive tract is defined as a geological setting that is considered to have potential for hosting a particular deposit type. To produce a probability distribution for contained gold within a permissive tract, the Three-part Assessment combines expert estimates for the number of undiscovered deposits with a representative grade-tonnage model (Singer 1993; Singer and Menzie 2010). The existing global low-sulfide gold-quartz vein grade-tonnage model (Bliss 1986) suffers from its antiquity, and thus poorly represents the significant Yilgarn greenfield and brownfield discoveries made during the late 1980s through to present day (Davies et al. 2018). Updating the global grade-tonnage model is recognised as a significant challenging task, specifically sourcing of reliable data from major gold-producing countries with limited public reporting, such as China and Russia (Davies et al. 2019b). Given the broad nature of global grade-tonnage models, and the difficulties associated with collecting comprehensive global data, it can often be preferable to develop a local grade-tonnage model (e.g. Lisitsin et al. 2014).

When the global model does not match the grade-tonnage properties of local deposits, a local model can provide geologic setting- and scale-appropriate data for the mineral system and its characteristics. Such locally derived models consist of deposits determined to contain a similar metal association and style of mineralisation, and likely to have formed as part of the same mineralising system. As such, a further challenge in the application of the Three-part Assessment is the selection of truly representative deposits to form a local grade-tonnage model.

In this study, the Three-part Assessment was applied in the estimation of orogenic gold endowment for the Archean Sandstone Greenstone Belt, located in the Yilgarn Block of Western Australia. Whereas previous assessments of the belt have relied upon dated or

CONTACT Rhys S. Davies rhyssamuel.davies@research.uwa.edu.au Centre for Exploration Targeting, School of Earth Sciences, The University of Western Australia, 35 Stirling Highway, Crawley, WA 6009, Australia

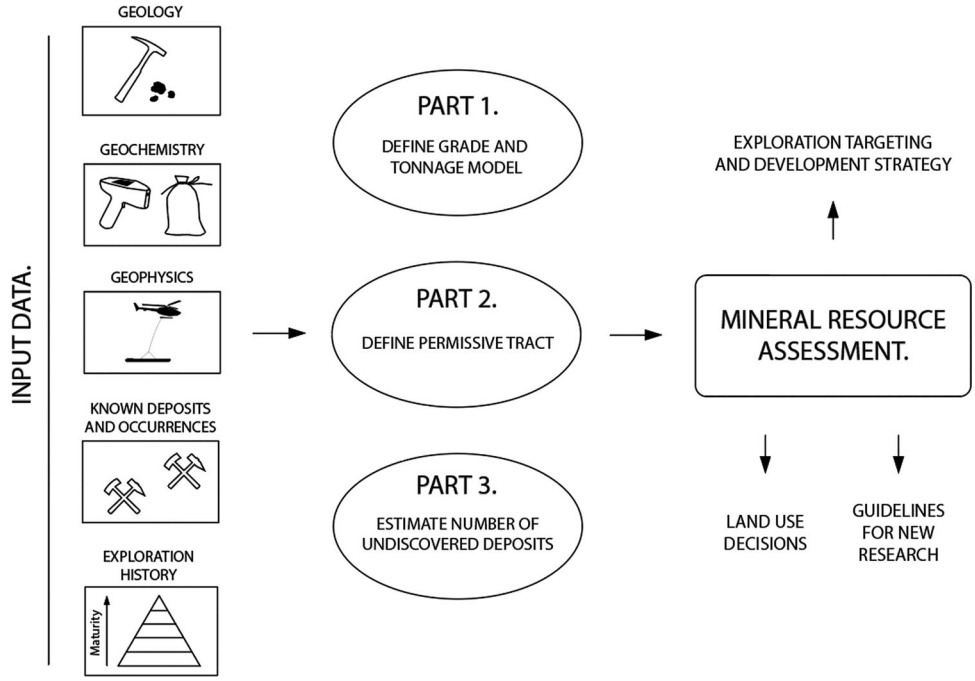

Figure 1. Three-part Mineral Resource Assessment framework outlining assessment stages and data input (modified from Singer 1993).

expert-derived grade-tonnage models (Davies et al. 2019b), this study utilises a suite of Yilgarn-specific orogenic gold grade-tonnage models. Specific models were developed through comprehensive review of historical exploration, resource and production data, for all known orogenic gold deposits within the Yilgarn Block. Subsequently, the total population of gold deposits was separated to represent several individual terranes within the Yilgarn Block, of contrasting gold endowment, potentially representing different mineralising systems or similar systems that operated within different lithostratigraphic or structural domains at slightly different times, but within the same geodynamic setting.

Background

Orogenic gold systems

Several authors have recognised that individual deposit models form part of a much larger Earth system, with many shared processes aligning to form ore deposits (Kerrich et al. 2005; Reddy and Evans 2009; McCuaig et al. 2010; Hronsky 2011; Cawood and Hawkesworth 2015; Hagemann et al. 2016). Goldfarb and Groves (2015) outlined the spatial distribution of gold forming systems (Figure 2), with Hronsky et al. (2012) defining constituent ore forming processes (Figure 3), and relating these to features that can be mapped directly in spatial geoscience datasets (Table 1). It is recognised that several aspects of fertility, geodynamics and whole-lithospheric architecture are likely to be shared across provincial and continental scales, whereas at the camp to ore-shoot scale, elements of ore formation result in local variations. Despite these local variations, orogenic gold deposits (Goldfarb et al. (2005) and references therein) have been recognised to share a common set of geological characteristics. These include a spatial relationship to regional trans-lithosphere structures; structural control of mineralisation at deposit scale; low-salinity aqueous-carbonic fluid compositions; similar mineral alteration assemblages, which vary systematically with host rocks and metamorphic setting; and formation at syn- to post-peak metamorphic temperatures along a crustal continuum between 180C and 1 kbar and >700C and 5 kbar (Groves 1993).

Although significant progress has been made in understanding ore formation and common deposit characteristics, a lack of clarity remains as to exactly how the critical system elements influence regional endowment and the grade-tonnage characteristics of resulting gold deposits.

Regional geological setting

The Archaean Yilgarn Block of Western Australia (Figure 4) is widely thought to have evolved through Neoarchean subduction, arc magmatism and accretion of outboard terranes on to a tectonic foreland (Krapez and Barley 2008, and references therein).

The age and lithospheric structure of the Yilgarn Block is segmented (Figure 5), as revealed by a regional, craton-wide epsilon Nd map from Mole et al. (2013). The Yilgarn is heterogeneous, comprising juxtaposed terranes defined by their contrasting terrane-scale geological and isotopic characteristics. The Yilgarn Block is therefore subdivided into seven terranes (Figure 4),

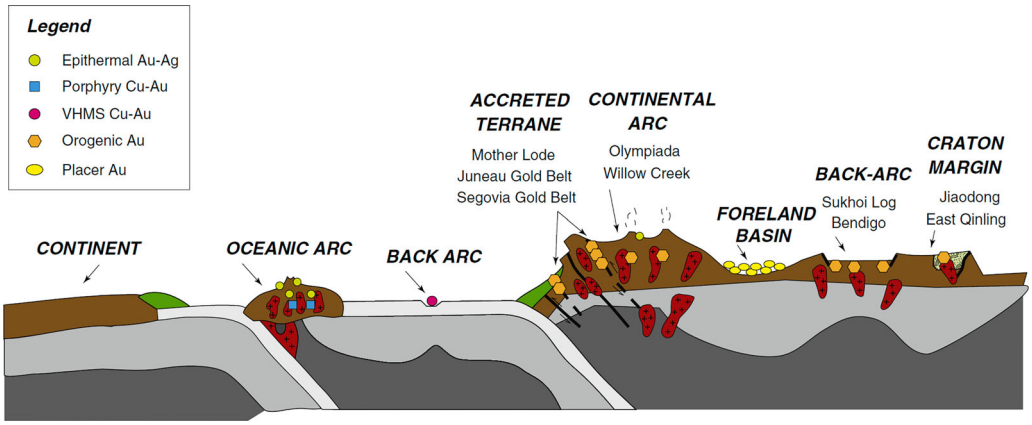

Figure 2. Tectonic settings of orogenic and other gold deposit types (after Goldfarb and Groves 2015).

four of which form the Eastern Goldfields Superterrane (EGS). The Youanmi Terrane, to the west, and the EGS consist of NNW-N-trending greenstone belts with intervening extensive granite batholiths or domes (Cassidy 2006). The Youanmi Terrane contrasts markedly with the terranes to the east in terms of its more negative epsilon Nd values that indicate older lithosphere compared to the more juvenile lithosphere of the Kalgoorlie and Kurnalpi Terranes (Figures 4 and 5). Evidence presented by Van Kranendonk et al. (2013), suggests that from *circa* 2.7 Ga the Youanmi Terrane and the EGS evolved as a single crustal element affected by Neoarchean plume-related magmatism and rifting (Table 2). For a more detailed background, the Yilgarn Block and its constituent parts are described by Cassidy (2006), with the structural and magmatic evolution of the Yilgarn Block summarised by Vielreicher et al. (2015) and references therein. They show that although the evolution of the Kalgoorlie and Kurnalpi Terranes was essentially similar, events, including gold mineralisation, were approximately 10 my later in the Kurnalpi Terrane.

The Yilgarn Block is deemed prospective for Archaean orogenic gold mineralisation, with numerous deposits already defined through exploration (Guj et al. 2011) and annual production (2018) of approximately 200 t Au (DMIRS 2018).

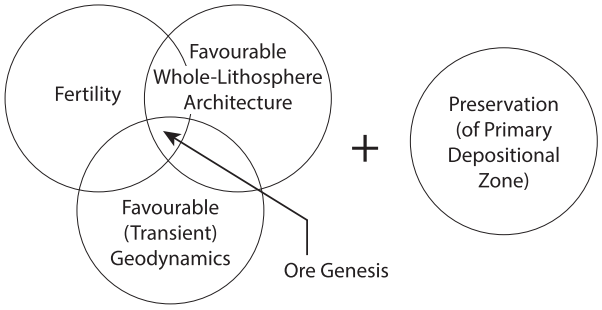

Figure 3. Critical elements of a mineral system (after McCuaig and Hronsky 2014).

Orogenic gold mineralisation occurred late in the structural history of the Yilgarn Block, between 2.66 and 2.63 Ga. This phase of mineral emplacement accompanied the development of anastomosing NNW- to NNE-striking trans-lithosphere structures, represented by brittle-ductile shear zones (Blewett and Czarnota 2007; Vielreicher et al. 2015). These structures are defined as D3 and D2/3 in the Youanmi Terrane and EGS, respectively (Table 3). Despite shared structural history, broadly similar timing of gold mineralisation, and likely large-scale orogenic gold system processes, the terranes of the Yilgarn Block appear to have contrasting gold endowments (Table 4).

Sandstone Greenstone Belt

The Sandstone Greenstone Belt covers approximately 920 km^2 in the north-eastern part of the Youanmi Terrane (Davies et al. 2018: Figure 6). The geomorphology of the belt comprises BIF ridges cropping out along the eastern and western flanks, and considerable recent cover and deep paleochannels throughout the centre of the belt.

The western edge of the belt abuts the north-eastern section of the NE-striking first-order Youanmi Shear Zone, whereas the eastern side of the belt abuts the NW-striking first-order Edale Shear Zone. The Edale Shear Zone is continuous to the southeast, but merges with the Youanmi Shear Zone at the northern tip of the belt to form an arrowhead geometry (Davies et al. 2017).

The lithostratigraphy of the belt is similar to other Yilgarn greenstone belts, including those of the EGS (Chen 2005). However, correlation is difficult due to limited geochronological data (Chen et al. 2006). The belt is characterised by low-strain, greenschist-facies metamorphism of mafic, ultramafic and minor sedimentary successions, with limited outcrop as a significant proportion of the belt is covered by a thick regolith profile (Davies et al. 2017: Figure 6). The central-

Table 1. Critical and constituent elements in the formation of gold deposits (after McCuaig et al. 2010).

		Critical elements			
		Fertility	Favourable geodynamics	Favourable architecture	Primary depositional zone
Scale	**Ore-shoot**	N/A at this scale	N/A at this scale	Localised dilatant zone in conduit-hosting structure	Pressure drop and favourable substrate
	Deposit	N/A at this scale		Pipe-like rock volume more favourable for fluid exit pulse (either local structural complexity or pipe of more competent rock)	Upper 10 km of crust *at time of the mineralising event* where fluid pressure (+T, X) gradients are greatest; preserved through multiple orogenic cycles
	Camp	N/A at this scale	Period of low active tectonic strain: for example stress switch causing transient neutral stress state causing fluid system to self-organise; areas of greatest uplift provides stress switch and high rates of energy and mass transfer	Major heterogeneity: for example, cross-structure intersection along trend of inverted rift-axial (or rift-marginal) fault with associated physical seal such as antiformal culmination or unconformity	
	Province	Discrete gold-enriched upper lithospheric domain, particularly near its margins; potentially mantle lithosphere enriched by small volume partial melts prior to termination of orogeny	Terminal phase of syn-ore orogenic event: for example, the transition to insipient extension associated with the termination of collision and locus of subduction retreating oceanward	Inverted retroarc rift; preferably developed at a continental margin, or margin of deep mantle lithosphere root; long lived 'vertically accretive' structure	
	Continental	Currently unclear but the occurrence of the western US gold superprovince suggests that some control at this scale exists	A major collisional orogenic event within the historic of an evolving accretionary orogen; the major collision that actually terminates a long-lived (>200 my) is most prospective and normally associated with a peak of supercontinent formation	Major subcontinental scale lineament representing long-lived zone of transverse dislocation within accretionary orogeny; long lived 'vertically accretive' structure	

northern and outer flanks of the belt comprise massive to foliated basalts, intercalated with subordinate sedimentary units. To the south, the belt comprises poorly exposed ultramafic and high-magnesium mafic volcanic rocks and subvolcanic sills with interflow oxide-facies BIF. The northern apex of the belt comprises shale and siltstone, intercalated with BIF, chert and minor ultramafic rocks (Davies et al. 2019a). Additionally, a variety of granites (*sensu lato*) intrude the belt along granite-greenstone contacts and regional-scale ductile shear zones.

The first three phases of deformation experienced by the SSGB align closely with those recorded within greenstone belts across the Youanmi Terrane, and several minor post-D3 deformation phases are also recognised (Table 5). Although these late events represent only localised variations in the regional stress field, they appear to have a close relationship to gold mineralisation (Davies et al. 2018).

Gold deposits

For this application of the Three-part Assessment, only deposits containing over 0.8 t Au are considered as significant (Lisitsin et al. 2010, 2014). At the time of assessment, ten known orogenic gold deposits of over 0.8 t Au had been defined within the belt (Figure 6), with a total endowment of 59 t Au, comprising 38 t of historic production (from alluvial, shallow underground and open-pit operations) and 23 t in resources or reserves (Davies et al. 2019a: Table 6). Early discoveries such as Hacks, Oroya and Hancock's/Bull Oak occurred around the beginning of the twentieth century, with a second wave of discoveries, including Bulchina, Two Mile Hill and Lord Nelson, close to the end of the twentieth century (Davies et al. 2020b: Figure 7). Although significant exploration efforts have taken place in the belt (Figure 8), several areas remain untested, particularly for primary zone mineralisation in fresh bedrock. As a consequence, exploration within the belt continues to discover additional gold mineralisation and result in continuing brownfields resource growth (Middle Island Limited 2018; Alto Metals Limited 2019).

The geological characteristics of known deposits within the Sandstone Greenstone Belt are presented in Table 7. Mineralisation has been defined within almost all domains and lithologies in the Sandstone Greenstone Belt (Figure 6), and known deposits share several common features, including: high grade 'free' gold associated with thin quartz veins; strong brittle-ductile structural controls; similar hydrothermal alteration in greenschist-facies host rocks; relatively late timing of mineralisation; and highly effective, deep weathering processes, resulting in significant supergene enrichment (Davies et al. 2017). For a more detailed

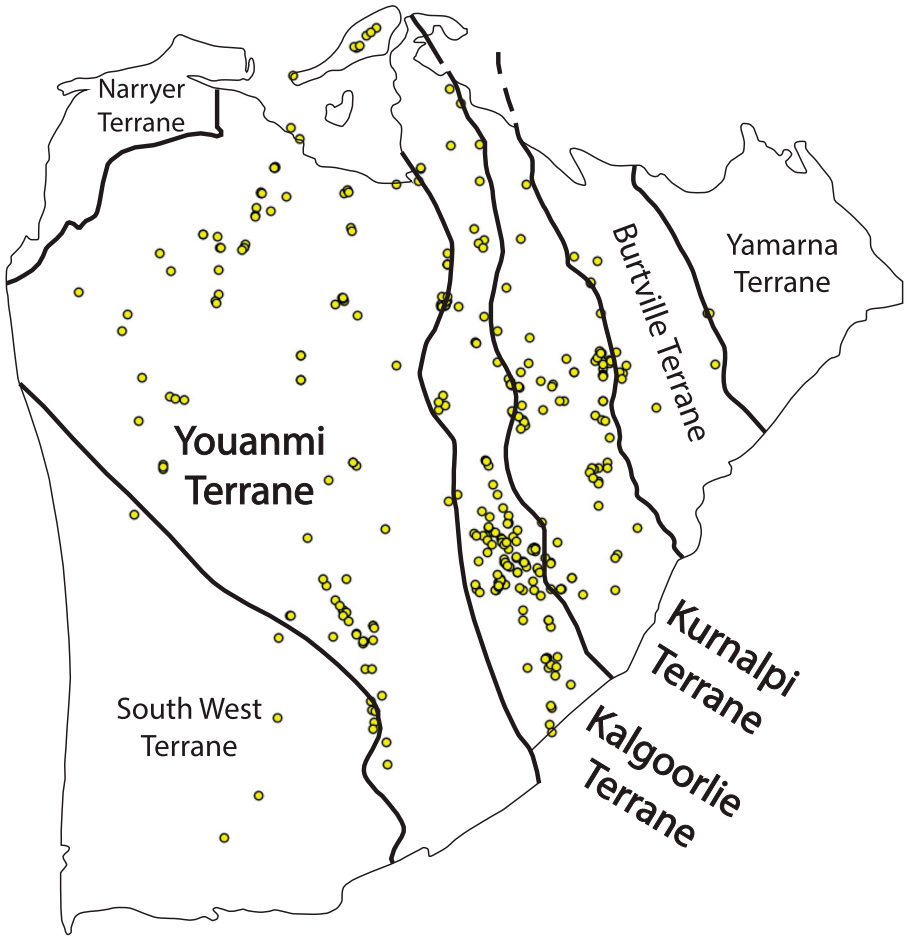

Figure 4. Terranes of the Yilgarn Block, showing gold deposits (yellow dots) utilised to produce the Yilgarn and Terrane-scale grade-tonnage models.

description of geology, historic exploration activities, and the existing mineral endowment of the Sandstone Greenstone Belt, the reader is directed to Davies et al. (2018).

Method

The USGS Three-part Undiscovered Mineral Resource Assessment provides an estimate of the number and quality of undiscovered deposits within a given region. The basic concepts of the Assessment were initially developed at the USGS (Singer 1975) and have since been applied at several scales, from global (Drew and Menzie 1993) to province (Lisitsin et al. 2014), and for several commodities including nickel (Rasilainen et al. 2016), copper (Hammarstrom et al. 2005) and gold (Lisitsin et al. 2014).

The Assessment comprises three separate stages (Figure 1), before the results are combined to produce a probabilistic estimate of mineral endowment. These stages are: (1) the selection or definition of an appropriate grade-tonnage model, specific to a particular mineral deposit type, that is considered representative of the potential grade and tonnage of undiscovered deposits in the study area; (2) definition of a permissive tract of land, within the study area, with potential to host the deposit type being assessed; and (3) estimation of the total number of deposits, representative of the grade and tonnage model selected, that exist within the defined permissive tract (Singer and Menzie 2010).

Part 1: development of grade-tonnage model

The definition of a deposit type, in this case orogenic gold (as defined by Groves et al. 1998; Goldfarb et al. 2005), helps the exploration geologist focus on relevant geological settings in which deposits are likely to have formed. Combined with a representative grade-tonnage model, this information provides constraints on the potential number of deposits in a given area and their likely grade and tonnage characteristics (Singer and Menzie 2010). Where an appropriate global grade-tonnage model is not available, a local model is developed through collection of comprehensive grade and tonnage data for all relevant known deposits within a geologically defined region.

The existing global low-sulfide gold-quartz vein grade-tonnage model was developed by J.D. Bliss in 1986. This model is deemed to now be dated due to significant new discoveries and additional brownfields resource growth that have taken place between the early 1980s and present day. This period resulted in a

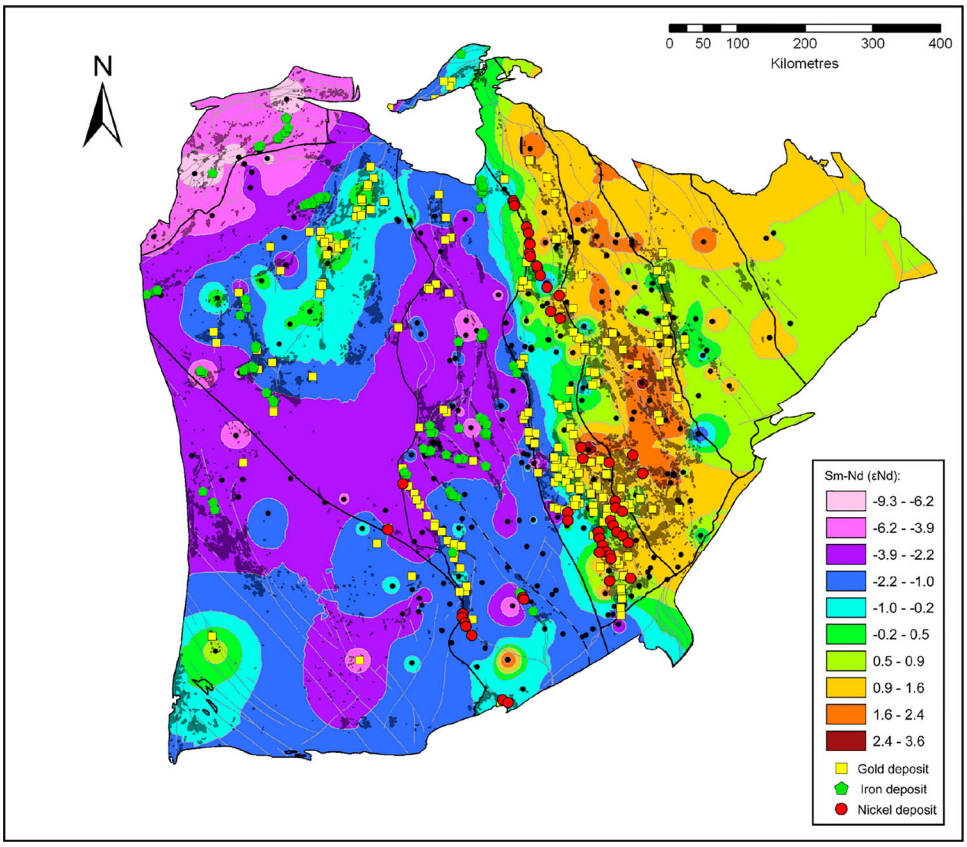

Figure 5. Epsilon neodymium isotopic map of the Yilgarn block, Western Australia at 2.7–2.6 Ga, showing distribution of ca. 2.7 Ga world-class komatiite-associated Ni-Cu deposits, ca. 2.65 Ga world-class orogenic gold deposits, and BIF-hosted iron oxide deposits. Isotopic maps enable imaging of whole lithosphere architecture through time, with the strong N-NW-trending gradient in the centre of the figure interpreted to be the margin of the proto-craton at ca. 2.7 Ga. Evolved crust is present to the west and juvenile crust to the east (after Mole et al. 2013).

suite of new discoveries within the Yilgarn Block (Figure 9), as well as much of the rest of the world; including Canada (Ellefsen 2019) and China (Zhang et al. 2015). As a result, this study utilises several updated Yilgarn-specific grade-tonnage models, based on data from 346 deposits compiled by MinEx Consulting as part of a larger global deposit database.

The MinEx Consulting database contains data on deposit type, age, discovery, and size; based on historic production, resources and reserves. Development of the MinEx deposit database has comprised comprehensive review of company public reports (e.g. annual reports, press releases and JORC/NI 43-101 resource studies), technical and trade journals (e.g. *Economic Geology*, *Northern Miner* and *Mining Journal*), government files (e.g. Western Australian Department of Mines and Petroleum) and personal communications with industry contacts.

As with previous Three-part Assessments, only gold deposits containing over 0.8 t original contained Au were included, and multiple deposits within 1.6 km were treated as part of the same mineralising system and aggregated into a single camp. That is, aggregation of deposits within 1.6 km was conducted in line with Singer and Menzie (2010), under the assumption that these deposits likely belong to the same system and

Table 2. Summary of features of the terranes of the Yilgarn Block (modified from Cassidy 2006). EGS = Eastern Goldfields Superterrane.

Terrane		Age of initial crust formation (Ga)	Depositional ages of greenstones (Ga)	Emplacement ages of granites and gneisses (Ga)	Age of deformation and metamorphism (Ga)
Narryer Terrane		3.8-3.4	?3.73	3.73-3.6, 3.48, 3.3, 3.0, 2.75, 2.68-2.62	c. 3.3,?2.75, 2.68-2.62
South West Terrane		?3.5-3.0	?3.0,?2.8, 2.7	?3.2, 2.8, 2.68-2.62	?2.68-2.62
Youanmi Terrane		?3.4-2.9	3.01-2.92, 2.81, 2.76-2.72	3.01-2.92, 2.81, 2.76-2.68, 2.66-2.62	>2.74-2.68, 2.66-2.63
EGS	Kalgoorlie Terrane	?3.0-2.8	?2.94,?2.81, 2.74-2.66	2.81, 2.75-2.74, 2.68-2.66, 2.65-2.63	2.67-2.63
	Kurnalpi Terrane (western domains)	2.9-2.8	2.71-2.68	2.7, 2.68-2.66, 2.65-2.63	2.67-2.63
	Kurnalpi Terrane (eastern domains)	?3.1-2.9	>2.8, 2.72-2.68	?2.95, 2.71, 2.68-2.66, 2.65-2.63	2.67-2.63
	Burtville Terrane	?3.0-2.8	2.81, 2.77-2.66	?2.95, 2.8-2.77, 2.69-2.63	?2.67-2.63

Table 3. Summary of deformation events of the Yilgarn Block (modified from Chen 2003).

Youanmi Terrane	Eastern Goldfields Superterrane	Timescale
D1 N-S compression: E-trending folds		Ca. 3.0 Ga
D2 E-W compression: upright folds, foliation, and gneissic banding	D1 N-S compression: thrusts, recumbent folds	Ca. 2.7 Ga
D3 E-W compression: NE- and NNE-trending dextral shear zones	D2: ENE-WSW shortening: upright folds, thrusts, foliation D3 E-W transpression: NNE-trending sinistral shear zones	Ca. 2.67 Ga

have been mined separately for economic reasons. A cut-off of 0.8 t Au was applied in line with Lisitsin et al. (2010), as deposits of < 0.8 t gold are considered to be of limited economic relevance. Care was taken to include all smaller deposits in the local grade-tonnage model, as many deposits below 5.7 t (200,000 oz) gold remain unreported by larger mining companies due to limited economic significance to those particular organisations (R.C. Schodde pers. comms. 2018).

Although the MinEx database represents a thorough review of historic production, resources and reserves, many of the gold deposits featured in the grade-tonnage models remain uneconomic to mine. These deposits are included to provide a comprehensive distribution of potential deposit sizes, since many factors beyond grade and tonnage can influence whether a deposit is developed into a mine (such as depth, commodity price, mineral policy and land access), meaning total historic production of mines is not necessarily equal or representative of future production (Ellefsen 2019). At times, deposits are reported under different names and occasionally production has been aggregated into a broad mining camp. Variations in grade-tonnage models due to modern mining techniques can also influence the results of a Three-Part Assessment. With the development of modern mining techniques average grades of orogenic gold deposits have dropped drastically, which in-turn has increased average ore tonnage (Davies et al. 2019b). Owing to these considerations, all deposits in the database were subjected to a comprehensive data-cleansing and validation process. Considerable effort ensured consistency and comparability of reported gold grades and tonnages over time. Where possible, past production was attributed as contained gold, or at least combined with subsequently delineated resources, and resources are compared by selecting a common and consistently low cut-off grade where available.

Initially a Yilgarn Block grade-tonnage model was developed from all 346 gold deposits in the MinEx database. Grade and tonnage distributions for the Yilgarn Block model are presented in Figure 10, and log-normal parameters are provided in Table 8. Subsequently, in order to explore the potentially more-local variations in gold endowment based on contrasts between well-defined components of the Yilgarn Block (Figure 4), three terrane-scale grade-tonnage models were produced as a sub-set of the MinEx database. These are, from east to west, the Youanmi Terrane (100 deposits), Kalgoorlie Terrane (146 deposits) and Kurnalpi Terrane (74 deposits) grade-tonnage models. Their grade and tonnage log-normal distribution parameters are presented in Table 8, and log–log plots of their respective deposit size distributions are provided in Figure 11.

The contrasting grade-tonnage models relate to a number of contrasts in critical parameters for broadly similar orogenic gold mineral systems in each Terrane. These include: (1) the older lithosphere for the Youanmi Terrane versus the other Terranes (Figure 5): (2) the narrower, higher metamorphic-grade greenstone belts of the Youanmi Terrane compared to the more-extensive, lower metamorphic-grade greenstone belts of the other Terranes; (3) differences in the dominant host rocks, from thick differentiated dolerite sills in the Kalgoorlie Terrane, to granite-sedimentary rock contacts in the Kurnalpi Terrane, to thin BIF units and shear zones in ultramafic rock units in the Youanmi Terrane; and (4) the slightly younger age of gold mineralisation in the Kalgoorlie Terrane relative to the Kurnalpi Terrane (Vielreicher et al. 2015), with the age of gold mineralisation in the Youanmi Terrane equivocal.

Table 4. Summary statistics for gold deposits of the Yilgarn Block, Youanmi Terrane, Kalgoorlie Terrane, Kurnalpi Terrane, and Sandstone Greenstone Belt.

	Yilgarn Block	Youanmi Terrane	Kalgoorlie Terrane	Kurnalpi Terrane	Sandstone Greenstone Belt
Count	346	100	146	74	12
Sum (t Au)	13441.16	2204.91	8584.70	2130.06	57.19
Mean (t Au)	38.85	22.05	58.80	28.78	4.77
Standard Error	8.31	4.47	18.87	8.53	1.18
Median (t Au)	8.99	8.87	9.05	8.91	3.35
Standard Deviation	154.58	44.65	228.01	73.39	4.08
Sample Variance	23896.22	1993.83	51989.99	5386.40	16.63
Kurtosis	225.80	26.49	110.91	34.00	0.55
Skewness	13.84	4.74	9.98	5.41	1.01
Range (t Au)	2615.65	324.96	2615.61	539.70	13.02
Minimum (t Au)	0.86	0.89	0.90	0.86	0.87
Maximum (t Au)	2616.51	325.85	2616.51	540.56	13.89

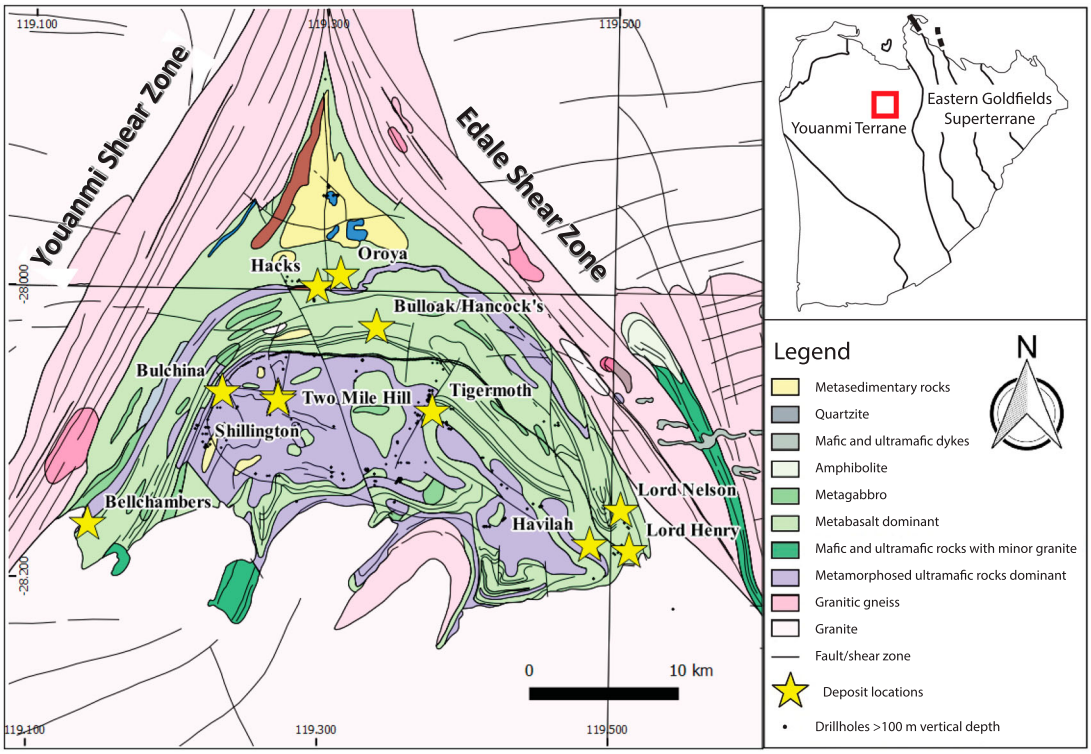

Figure 6. Regional-scale interpreted bedrock geological map of the Sandstone Greenstone Belt, outlining major gold deposits and drill holes exceeding 100 m in depth (Davies et al. 2018). The defined permissive tract comprises all lithological units mapped within the Sandstone Greenstone Belt, and does not include granitic rocks residing outside of the greenstone belt.

Part 2: definition of permissive tract

Permissive tracts are defined by a geological setting considered to have potential for hosting the selected deposit type (Singer and Menzie 2010). Although a small number of orogenic gold deposits within the Yilgarn Block are hosted by granite intrusions external to the greenstone belts (e.g. Golden Cities: Harjinder et al. 1999), these deposits are deemed

Table 5. Recognised regional and localised deformation phases for the Sandstone Greenstone Belt (after Davies et al. 2018).

Phase of deformation	Stress regime	Evidence	Timing
D1	Regional-scale N-S compression	Layer-parallel D1 foliation and D1 thrusts in tremolite-chlorite (-talc) schist, along with an east-striking, belt-scale D1 syncline, which have been overprinted by later structures (e.g. northerly trending F2 Sandstone Syncline) to produce type-2 and type-3 fold interface patterns. Initiation of the Sandstone Decollement was most likley a product of D1 thrusting	Ca. 3.0 Ga
D2	Progressive E-W and SE-NW constriction	Macroscopic folds with NW-striking axial planes and north-plunging fold axes. Refolded D1 folds in the northern half of the Ultramafic Domain, produced northerly trending gneissic banding, and potentially formed periclinal Sandstone Syncline to portray box-fold geometry. Constriction of the northern Sedimentary Domain may have been a product of D2 deformation	Ca. 2.7 Ga
D3	Progressive (from D2) inhomogeneous E-W shortening	Kilometres wide, east-trending, sinistral Edale Shear Zone and the northeast-trending, dextral Youanmi Shear Zone. The initiation of the WNW-striking Dandaraga Fault as a sinistral shear, although the majority of its evolution is likley to have occurred during subsequent deformation events	Ca. 2.67 Ga
D4	Localised strain heterogeneity due to diapiric build-up of small volume granitoid pluton	Open to closed antiforms and tight to isoclinal synforms along the southern margin of the belt, with NNE-striking subvertical axial planes and gentle north-plunging fold axes. Transcurrent flextural-slip deformation along the Sandstone Decollement in response to differential strain-rates between the Mafic and Ultramafic Domains	Unknown
D5	Localised strain heterogeneity due to E-W directed stress field during waning stage of D4	Major fault corridor along N-S and WNW orientations, many of which are intruded by small-scale felsic intrusions. The WNW-striking Dandarage Fault system would have continued to deform in a sinistral manner and it is inferred that the N-S striking, gently dipping, laminated reef-style gold deposits and the steeply dipping, shear zone-hosted lode-gold deposits were deposited during this event	Unknown
D6	Continued E-W compression during cratonisation at the end of the Archaean	Fissue-like eruptions of doleritic magma to form the E-W trending dolerite dykes evident in the aeromagnetic data	?

Table 6. Deposits of Sandstone Greenstone Belt, showing historical gold production and resources in tonnes, listed in decreasing order of total gold resource (after Davies et al. 2019b). Data pre-1954 was calculated from historical records (Davies et al. 2018) and post-1954 was sourced from Troy Resources internal reports (Lowe and Ross 2007; Maddocks et al. 2009). Note that Vanguard and Indomitable resources increased to current values with the release of a resource estimate by Alto Metals Ltd. in June 2019 (Alto Metals Limited 2019), after the expert assessment described here had taken place. This explains the discrepancy between known number of deposits at the time of the assessment ($n = 10$) and the present day number ($n = 12$).

Deposit	Historical Production (t gold)	Inferred Resources (t gold)	Indicated Resources (t gold)	Total Tonnes Gold
Two Mile Hill	0.57 (20,000)	12.81 (452,000)	0.51 (18,000)	13.89 (490,000)
Oroya	7.17 (253,000)	0.28 (10,000)	0	8.18 (263,000)
Lord Nelson	6.44 (207,000)	0.14 (5,000)	1.15 (37,000)	7.74 (249,000)
Hacks	7.34 (236,000)	0	0	7.34 (236,000)
Bulchina	7.15 (230,000)	0	0	7.15 (230,000)
Lord Henry	1.77 (57,000)	0.06 (2,000)	1.80 (58,000)	3.64 (117,000)
Bull Oak	2.49 (80,000)	0.56 (18,000)	0	3.05 (98,000)
Havilah	1.06 (34,000)	0.06 (2,000)	0.47 (15,000)	1.59 (51,000)
Vanguard	0	0	1.56 (50,000)	1.56 (50,000)
Indomitable	0	0	1.28 (41,000)	1.28 (41,000)
Shillington	0.72 (23,000)	0	0.19 (6,000)	0.90 (29,000)
Tigermoth	0	0	0.87 (28,000)	0.87 (28,000)
Wiraminna	0	0.72 (23,000)	0	0.72 (23,000)
Maninga Marley	0.40 (13,000)	0.25 (8,000)	0	0.65 (21,000)
Twin Shafts	0.62 (20,000)	0	0	0.62 (20,000)
Goat Farm	0.59 (19,000)	0	0	0.59 (19,000)
Bellchambers	0.06 (2,000)	0.44 (14,000)	0	0.50 (16,000)
Plum Pudding	0.31 (10,000)	0.07 (2,500)	0	0.039 (12,500)
Ladybird	0	0.09 (3,000)	0.28 (9,000)	0.37 (12,000)
Piper	0	0	0.14 (5,000)	0.14 (5,000)
Sandstone North	0	0.14 (5,000)	0	0.14 (5,000)
55 North	0.11 (4,000)	0	0	0.11 (4,000)
Wanderie	0.09 (3,000)	0	0	0.09 (3,000)
Eureka	0.06 (2,000)	0	0	0.06 (2,000)
Bulletin	0.03 (1,000)	0	0	0.03 (1,000)
Total	**37.76 (1,214,000)**	**16.94 (544,500)**	**8.30 (267,000)**	**63.00 (2,025,500)**

negligible in terms of total endowment (Guj et al. 2011) and are excluded from this study. In addition, the known orogenic gold deposits of the Sandstone Greenstone Belt are hosted within almost all rock types exposed within the belt (Davies et al. 2017, 2018; Jia et al. 2020). Thus, the delineation of the permissive tract for this study involved defining the extent of the 920 km^2 Sandstone Greenstone Belt (Figure 6) from regional geophysical survey data (Dentith and Mudge 2014).

Part 3: estimation of deposit numbers

The Three-part Assessment combines grade-tonnage data with expert estimates for the number of undiscovered mineral deposits (Singer and Menzie 2010). Here, experts are defined as having a minimum of ten years gold exploration-relevant experience, and were carefully selected to be impartial and independent of the area under assessment. Estimates were made during an interactive group workshop. During this workshop,

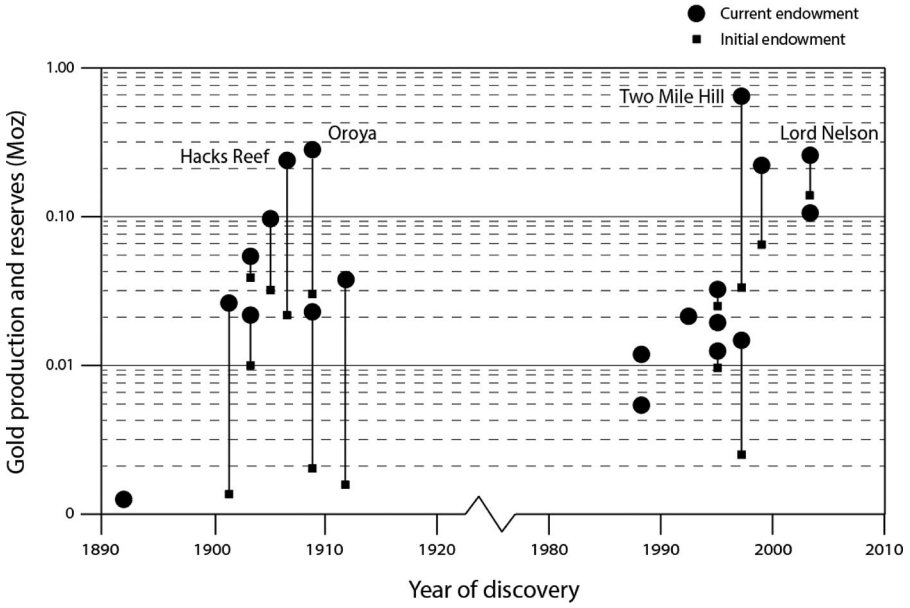

Figure 7. Year of discovery of gold deposits in the Sandstone Greenstone Belt, illustrating that new concepts and technologies can rejuvenate discovery in a previously mature region (after Davies et al. 2020b). During the initial gold rush, prior to WWI, gold discoveries were made based on evidence of mineralisation preserved in outcrop. A second wave of discoveries were made during the Western Australian 'heyday' of the 1980–2000s, through application of emerging concepts and technologies such as low-cost RAB drilling and geochemical sampling of regolith, with low-level (ppb) Au analysis, to define regolith-related dispersion. Although many of the deposits discovered post-1980 were in close proximity to existing deposits, they lacked evidence of mineralisation in outcrop, essentially representing a new exploration 'search space.'

eight experts were presented with the suite of comprehensive geoscientific datasets outlined in Table 9 (in digital and print-form) for the Sandstone Greenstone Belt (Figure 7), along with the series of four Yilgarn-specific grade-tonnage models (Figure 4 and Table 8). As per previous applications of the Three-Part Assessment (Singer 1993; Lisitsin et al. 2010, 2014), discussion was allowed during the group workshop. Although discussion and group interaction maximise individual and collective knowledge, the experts were required to produce individual and confidential estimates. No attempts were made to reach a group consensus, as this risks the introduction of behavioural aggregation, psychological biases, and promotes underestimation of uncertainty (Meyer and Booker 2001; O'Hagan et al. 2006).

Estimates were made in a probabilistic manner, such that: N50 is the median estimate, representing an equal (50%) chance that the true number of deposits is higher or lower than the estimate; N90 is the minimum estimate, where the expert is very confident (90%) that this number or more deposits exists; and N10 is the maximum estimate, where the expert believes there is a very low chance (10%) that this number or more deposits exists (Singer 1993). Importantly, these estimates must be consistent with the selected grade-tonnage model, such that half the total estimated number of deposits should contain greater than the median grade and tonnage (Singer and Menzie 2010). Expert estimates received equal weighting during the assessment process. As such, individual expert estimates were aggregated into a single distribution via the simple equal-weight linear-pooling method (Gedest and Zidek 1986; O'Hagan et al. 2006):

$$f(x) = \Sigma w_i f_i(x),$$

where $f(x)$ is the probability of a particular value for grade or tonnage; n is the total number of experts participating in the study; and w_i is $1/n$.

Monte Carlo simulation

The results are combined to provide exploration-relevant information, as, alone, the results of the three individual parts of the assessment are of limited use in exploration decision-making. To combine these results, a Monte Carlo simulation is used to produce a probability distribution function for contained gold within the permissive tract. This process is performed using the MAPMARK4 program (Ellefson 2017). For a detailed description of this programme, refer to Ellefson (2017) and Shapiro (2018).

For this study, percentile estimates for N5 and N1 were not produced, as N50 and N90 were estimated to be significantly higher than zero. N5 and N1 were assumed to be the same as N10, giving slightly lower overall estimates for total gold endowment. To maintain coherency and allow for comparison with the previous study conducted by Davies et al. (2019b), the MARK3 probability mass function (Root et al. 1992; Bawiec and Spanski 2012; Duval 2012) option was selected within the MAPMARK4 modelling software,

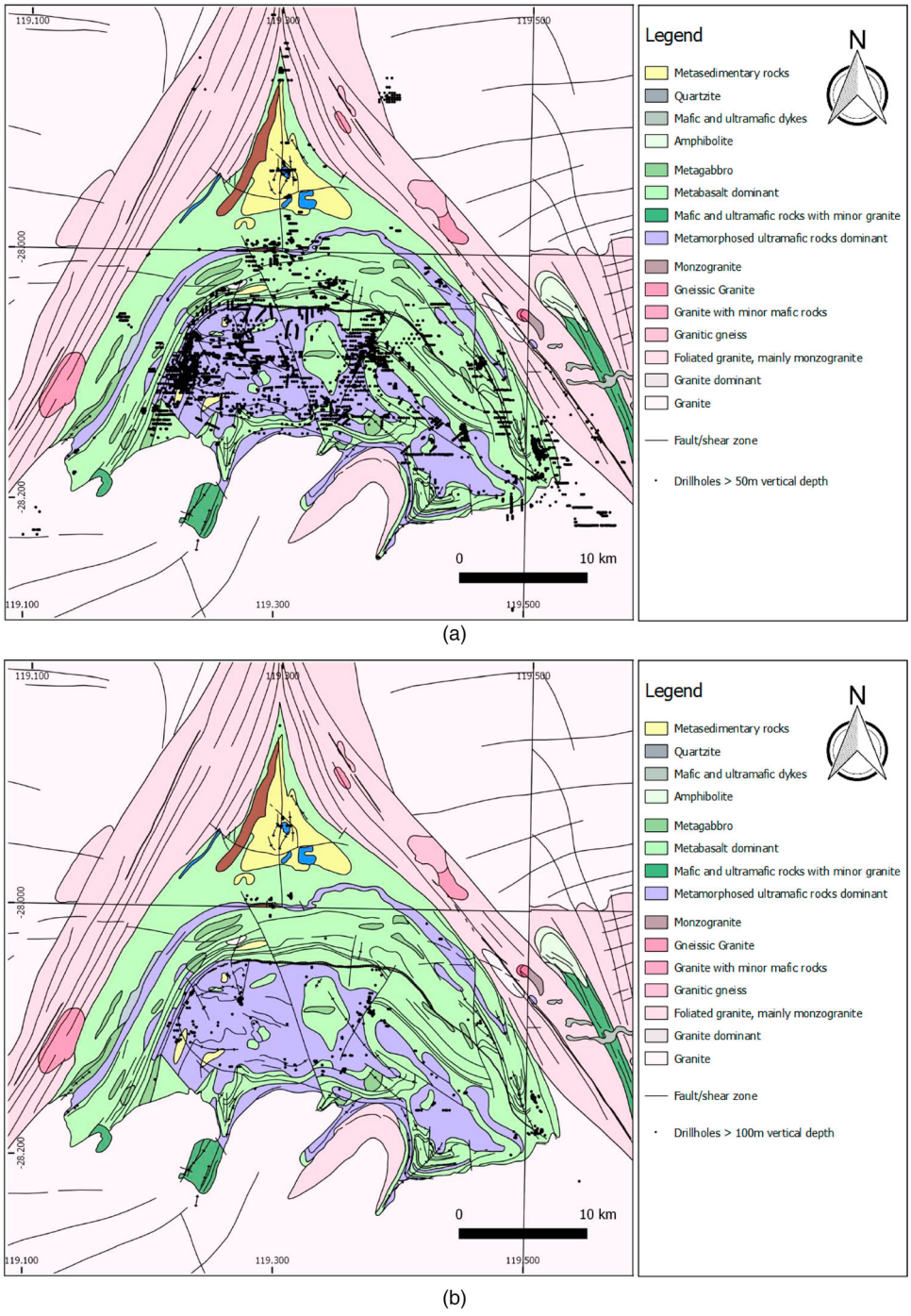

Figure 8. (A) Drill holes exceeding 50 m of vertical depth in the Sandstone Greenstone Belt (after Davies et al. 2018). (B) Drill holes exceeding 100 m of vertical depth in the Sandstone Greenstone Belt (after Davies et al. 2018). (C) Drill holes exceeding 200 m of vertical depth in the Sandstone Greenstone Belt (after Davies et al. 2018).

along with a truncated normal distribution type as the default recommended option (Ellefson 2017).

Results

Aggregated expert estimates for deposit numbers at N10, N50 and N90 are presented in Table 10 and individual estimates are presented in Figure 12. Although the experts were briefed several times that estimates for deposit numbers must align with the selected grade-tonnage model, the expert participants determined that their estimated deposit numbers would not materially differ between each of the three separate grade-tonnage models, given that ten deposits >0.8 t Au have already been discovered within the Sandstone Greenstone Belt.

Assessment results from Monte Carlo simulation are presented numerically in Table 11, and graphically in Figure 13. Utilising the Yilgarn-wide grade-tonnage model, this study predicts a total median gold endowment of 219 t gold and mean endowment of 225 t gold for the Sandstone Greenstone Belt. The Youanmi Terrane grade-tonnage model, arguably most appropriate for the Sandstone Greenstone

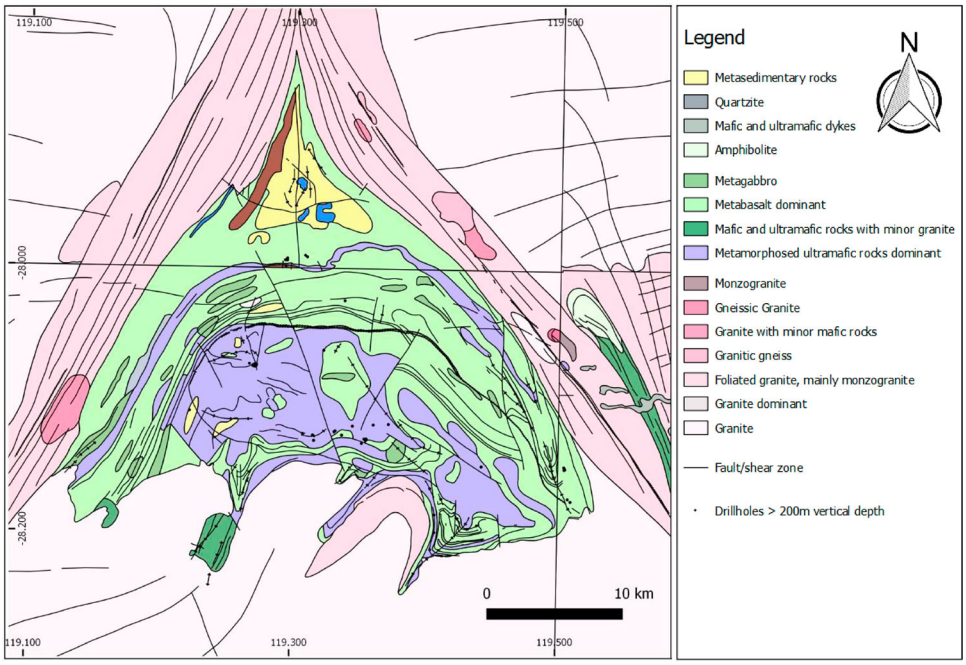

Figure 8 *Continued*

Belt, predicts a total median gold endowment of 166 t gold and mean endowment of 167 t gold. The Kalgoorlie Terrane grade-tonnage model, representing a highly endowed terrane to the east of Sandstone, predicts a total median gold endowment of 298 t gold and mean endowment of 319 t gold. The Kurnalpi Terrane grade-tonnage model, representing a moderately endowed terrane east of the Kalgoorlie Terrane, predicts similar results to the Youanmi Terrane grade-tonnage model, with a total median gold endowment of 179 t gold and mean endowment of 181 t gold. The four grade-tonnage models predict relatively similar P90 estimates for total gold endowment (ranging from 100 to 152 t), but present a greater range of predictions for P10 estimates (ranging from 241 to 510 t), as shown by probability and density distributions in Figure 13.

Discussion

Estimating the number and quality of undiscovered deposits, particularly those at great depth and beneath cover, represents a significant challenge for explorers in Western Australia (McCuaig and Hronsky 2014). By providing quantitative information regarding undiscovered mineral endowment, the USGS Three-part Mineral Resource Assessment is recognised as a valuable tool for guiding exploration decision-making.

The results of this Three-part Assessment, utilising several Yilgarn-specific grade-tonnage models, present a contrasting outcome to those produced by Davies et al. (2019b). In Davies et al. (2019b), an initial assessment, combining regression-derived estimates for the number of deposits with the 1986 global grade-tonnage model for low-sulfide vein-hosted gold (median total endowment of 33 t and mean of 130 t gold), was deemed to represent ore bodies that crop out or are buried beneath minimal *in-situ* cover. A more optimistic expert-derived estimate for the number and quality of undiscovered deposits (median of 210 t, mean of 220 t gold), based largely on empirical data, but influenced by the conceptual understanding of mineralising processes, provided a guide as to the potential endowment of the belt beneath transported cover and the deep *in-situ* weathering profile.

Here, expert estimates for deposit numbers are combined with Yilgarn-specific grade-tonnage models to provide a range of estimates for gold endowment. When comparing the expert estimates of Davies et al. (2019b) with the results presented here for the Yilgarn-wide grade-tonnage model, the predicted number of deposits and grade-tonnage distributions vary significantly. However, the resultant endowment estimates are similar (median of 210 and 219 t gold, mean of 220 and 225 t gold, respectively). In comparison, the terrane-based grade-tonnage models presented in this study provide a wide range of estimates for total endowment (median of 166–298 t, mean of 167–319 t gold), suggesting that careful selection of deposit populations for grade-tonnage models is required. These should clearly be selected based on the setting of the deposit populations, in terms of their lithosphere to terrane-scale setting.

Although underlying mechanisms leading to local variations in grade and tonnage characteristics are not completely understood, and exploration focus is likely to have some influence on grade-tonnage characteristics between terranes, this study clearly

Table 7. Key geological characteristics of gold mines in the Sandstone Greenstone Belt (after Davies et al. 2017).

Deposit	Host Structure	Strike	Dip	Local Structural Complexity	Host Rock	Veins	Alteration	Ore Assemblage
Two Mile Hill	N-S trending 722 Fault Zone	Subvertical stock	30° NW	Cross-cutting BIF units	Tonalite cross-cutting BIF and mafic volcanic rocks	Vein arrays and disseminated sulphide and gold in host rock	White mica-carbonate	Pyrite-galena-molybdenite-chalcopyrite-gold
Oroya	N-S trending shear zone?	N-S	30–45° W	E-W trending cross-cutting faults	Dolerite	Sulphide and gold in shear veins and vein arrays in host rock	White mica-carbonate	Pyrite-gold
Lord Nelson	NNW trending Trafalgar Shear Zone	NNW-SSE	50° W	W limb of NNW trending anticline	Granodiorite/basalt Ultramafic footwall	Sulphide and gold in shear veins	Actinolite-tremolite-chlorite-biotite	Pyrite-hematite-gold
Hack's Reef/ Black Range	N-S trending Hack's Creek Fault Zone	N-S	30–45° W	E-W trending cross-cutting faults and shale units	Dolerite contained by ferruginised graphitic shale units	Sulphide and gold in shear veins	White mica-carbonate	Pyrite-gold
Bulchina	NNE-trending Bulchina Shear Zone	NNE-SSW	30° W	Intersection of two regional shear zones Centre of NNE-trending anticline	Quartz porphyry Ultramafic footwall Dolerite hangingwall	Sulphide and gold in shear veins and vein arrays in host rock	Goethite-white mica-fuchsite-carbonate	Pyrite-gold
Lord Henry	ENE trending Trafalgar Shear Zone	ENE-WSW	30° N	NW trending cross-cutting faults Centre of NNE-trending syncline	Granodiorite Ultramafic footwall	Sulphide and gold in shear veins	White mica- chlorite	Pyrite-galena-arsenopyrite-sphalerite-chalcopyrite-gold
Bull Oak/ Hancock's	N-S trending 731 Fault Zone	NW-SE	30–40° NE	Cross-cutting BIF units	Granodiorite contained by BIF units Basalt footwall and hangingwall	Sulphide and gold in shear veins	White mica-carbonate	Pyrite-gold
Shillington	N-S trending 722 Fault Zone	NW-SE	30–60° NE	Intersection of N-S, NE and NW trending faults North flank of Nungarra dome	BIF flanked by dolerite wallrock	Shear veins and disseminated sulphide and gold in host rock	White mica-chlorite-carbonate-magnetite	Pyrite-gold
Maninga Marley	NW trending Trafalgar (?) Shear Zone	E-W	70° N	NE trending cross-cutting faults and granite/migmatite intrusions SW limb of NW trending syncline	Talc-chlorite-carbonate schist Ultramafic footwall Dolerite hangingwall	Sulphide and gold in shear veins and vein arrays in host rock	White mica-carbonate	Pyrite-gold
Bellchambers	NE trending shear zone	NE-SW	Subvertical	N-S trending cross-cutting structures	Black shale and basalt	Shear veins and disseminated sulphide and gold in host rock	White mica-carbonate?	Pyrite-gold?
Lady Hamilton	N-S trending 731 Fault Zone	NNE-SSW	45° W?	NE trending cross-cutting faults and BIF units	Basalt and ultramafic rock	Shear veins and disseminated sulphide and gold in host rock	White mica-fuchsite	Pyrite-gold

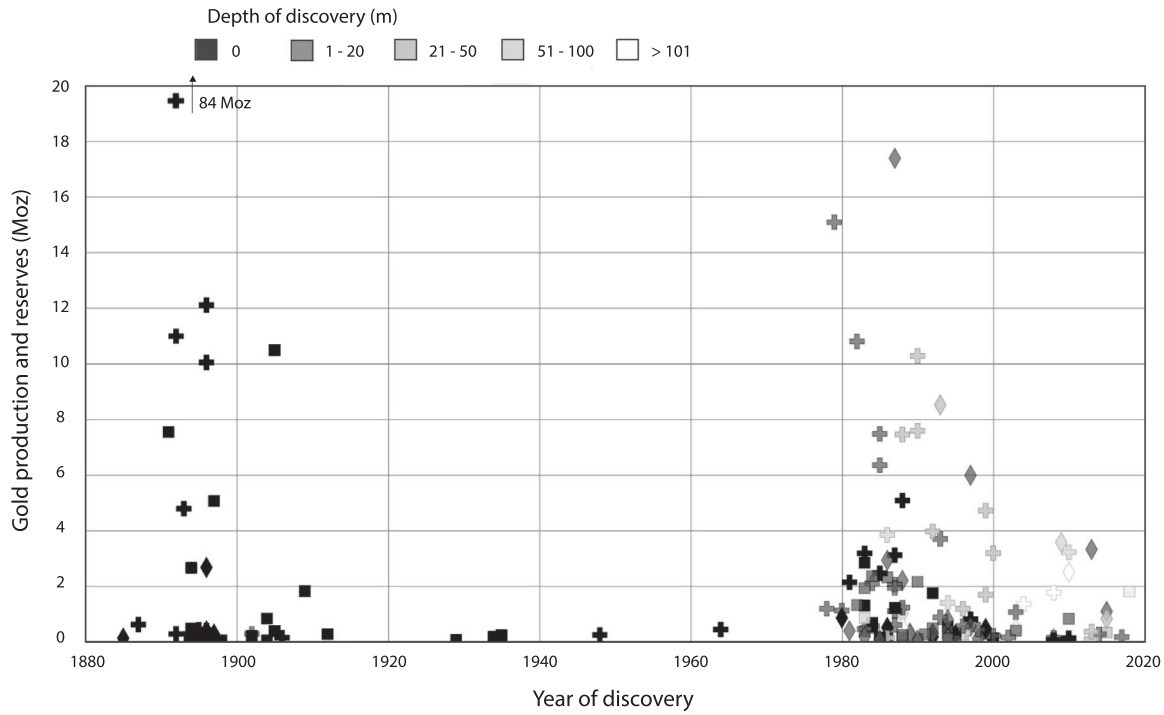

Figure 9. Year of discovery, size and depth of gold deposits in the Youanmi Terrane (squares), Kalgoorlie Terrane (crosses) and Kurnalpi Terrane (diamonds). During the initial gold rush, prior to WWI, gold discoveries were made based on evidence of mineralisation preserved in outcrop. A second wave of discoveries were made during the Western Australian 'heyday' of the 1980–2000s, through application of emerging concepts and technologies such as low-cost RAB drilling and geochemical sampling of regolith, with low-level (ppb) Au analysis, to define regolith-related dispersion. Although many of the deposits discovered post-1980 were in close proximity to existing deposits, they lacked evidence of mineralisation in outcrop, essentially representing a new exploration 'search space.'

demonstrates that orogenic gold deposits of significantly different grade-tonnage characteristics are concentrated in specific terranes within the Yilgarn Block, as expected from contrasts between terranes in parameters critical to the mineral systems of orogenic gold deposits (Groves et al. 2000). This presents a strong argument for the development of terrane-specific grade-tonnage models where sufficient data are available.

Further studies, including the development and comparison of craton- and terrane-specific grade-tonnage models, may help to direct geoscientific research towards elucidating as to which of the mineral system elements account for differences in grade-tonnage

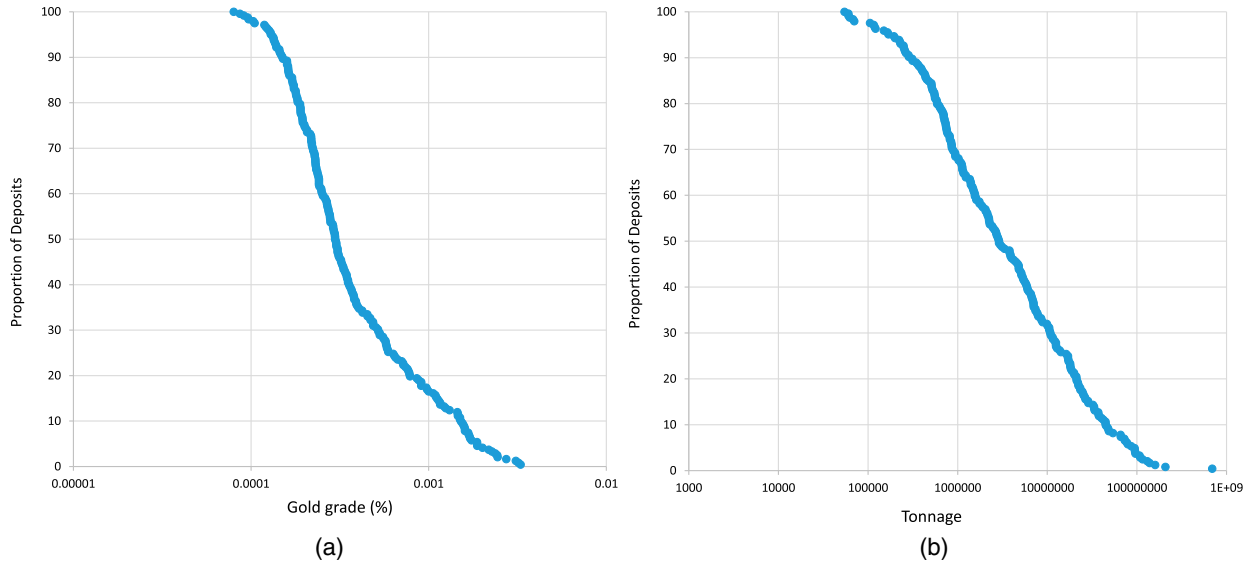

Figure 10. (A) Grade distribution of orogenic gold deposits of the Yilgarn Block. (B) Tonnage distribution of orogenic gold deposits of the Yilgarn Block.

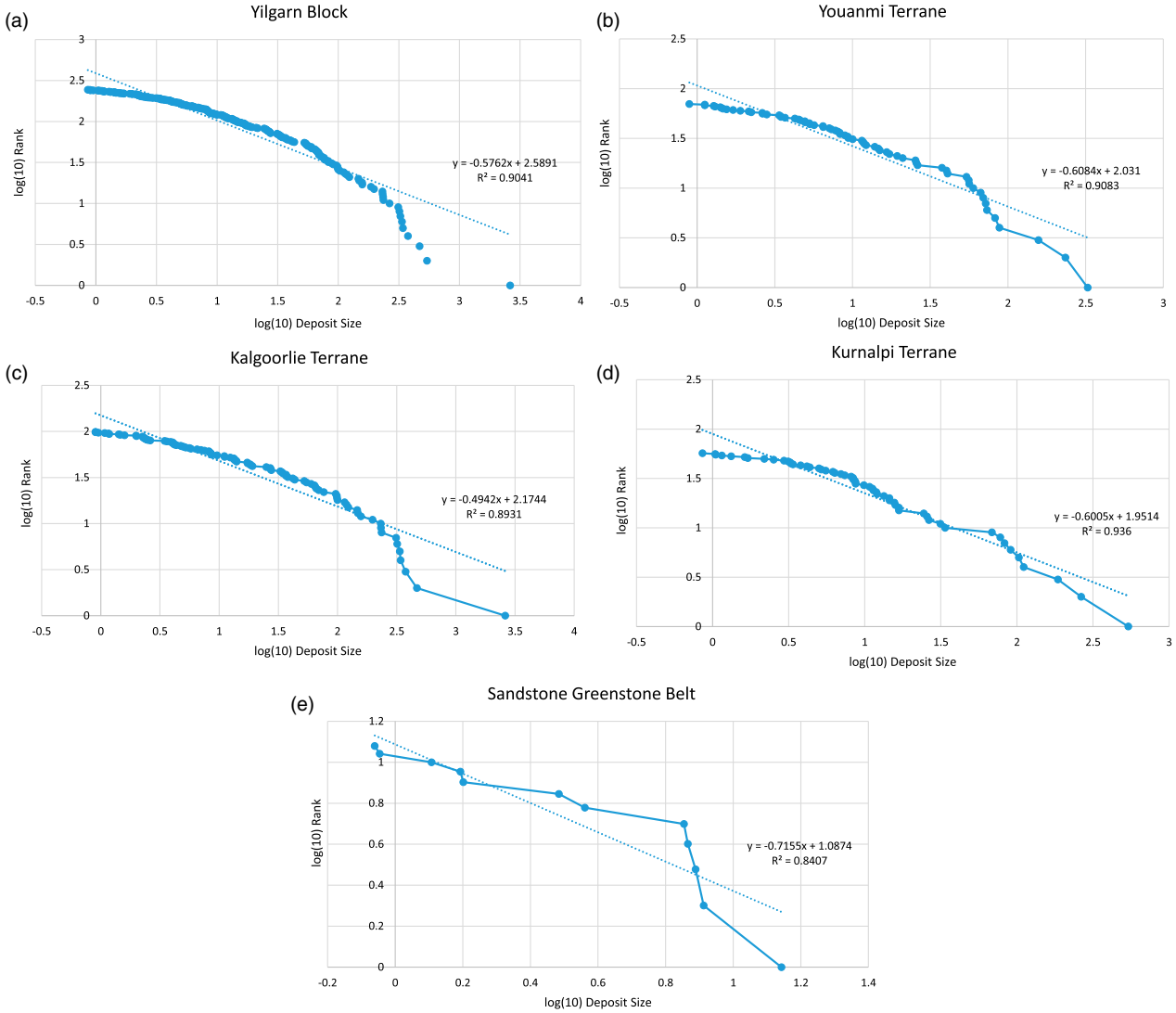

Figure 11. (A) Log–log plot of orogenic gold deposits of the Yilgarn Block, where the x-axis displays the logarithm (base 10) of the sizes of deposits, while the y-axis displays the logarithm (base 10) of their respective ranks. (B) Log–log plot of orogenic gold deposits of the Youanmi Terrane, where the x-axis displays the logarithm (base 10) of the sizes of deposits, while the y-axis displays the logarithm (base 10) of their respective ranks. (C) Log–log plot of orogenic gold deposits of the Kalgoorlie Terrane, where the x-axis displays the logarithm (base 10) of the sizes of deposits, while the y-axis displays the logarithm (base 10) of their respective ranks. (D) Log–log plot of orogenic gold deposits of the Kurnalpi Terrane, where the x-axis displays the logarithm (base 10) of the sizes of deposits, while the y-axis displays the logarithm (base 10) of their respective ranks. (E) Log–log plot of orogenic gold deposits of the Sandstone Greenstone Block, where the x-axis displays the logarithm (base 10) of the sizes of deposits, while the y-axis displays the logarithm (base 10) of their respective ranks.

Table 8. Parameters for the orogenic gold lognormal (base 10) grade and tonnage distributions, for the Yilgarn Block, Youanmi Terrane, Kalgoorlie Terrane and Kurnalpi Terrane. Values are presented as lognormal (base 10) to four significant figures, and where appropriate the true values are provided in brackets below.

	Yilgarn Block	Youanmi Terrane	Kalgoorlie Terrane	Kurnalpi Terrane
Number of deposits	346	100	146	74
Tonnage mean	7.1156	6.8312	7.2639	7.0438
	(13,050,000 t)	(6,780,000 t)	(18,360,000 t)	(11,060,000 t)
Tonnage variance	15.2944	14.4007	15.6042	14.8511
Tonnage P90	5.6335	5.3979	5.6902	5.6128
	(430,000 t)	(250,000 t)	(490,000 t)	(410,000 t)
Tonnage P50	6.2068	6.2122	6.2095	6.2175
	(1,610,000 t)	(1,630,000 t)	(1,620,000 t)	(1,650,000 t)
Tonnage P10	7.5153	7.2307	7.6621	7.3487
	(32,760,000 t)	(17,010,000 t)	(45,930,000 t)	(22,320,000 t)
Grade mean	0.7482	0.8264	0.7324	0.6922
	(5.6 g/t)	(6.7 g/t)	(5.4 g/t)	(4.9 g/t)
Grade variance	1.4080	1.5830	1.3317	1.2998
Grade P90				

(*Continued*)

Table 8. Continued.

	Yilgarn Block	Youanmi Terrane	Kalgoorlie Terrane	Kurnalpi Terrane
	0.2041 (1.6 g/t)	0.2788 (1.9 g/t)	0.2405 (1.7 g/t)	0.1492 (1.4 g/t)
Grade P50	0.7324 (5.4 g/t)	0.7356 (5.4 g/t)	0.7396 (5.5 g/t)	0.5302 (3.4 g/t)
Grade P10	1.0607 (11.5 g/t)	1.2095 (16.2 g/t)	1.9741 (9.4 g/t)	1.9827 (9.6 g/t)

Table 9. Datasets utilised by the experts in the Three-part Assessment of the Sandstone Greenstone Belt. These data are available from their respective Geological Survey of Western Australia repositories; WAROX, WACHEM, WAMEX, MINDEX and MAGIX (Riganti et al. (2015) and comprehensive references therein).

Datasets		Details
Geological mapping	1:50,000 scale	Outcrop/regolith mapping and basement interpretation (including stratigraphy and structural history)
Geological model		Coarse 3D interpretation of greenstone belt shell and major stratigraphic units
Drill holes	>18,000 collars	320,000 samples assayed (70% Au-only, 30% multi-element)
Surficial geochemical samples	>50,000 samples	80% soil, 10% rock chip, 8% auger, 1% stream sediment, 1% biogeochemistry
Petrophysics	>200 samples	Magnetic susceptibility, P-wave velocity, grain density, wet and dry bulk density, apparent porosity, and remnant magnetism (samples from 3 EIS diamond drill holes)
Airborne magnetometry and gamma-ray spectrometry		50–200 m line spacing, covering entire belt
Gravimetric		2–4 km (average 2.5) grid spacing, covering entire belt
Remote sensing		Landsat and ASTER covering the entire belt: full-colour drone photography for select regions within the belt
Seismic		One line crossing E-W across the belt: vibrators shooting 2–3 sweeps at spacing of 80 m or 40 m and receiver groups spaced 40 m apart along a 12 km spread.
Mineral deposits	24	Historical production and resources/reserves (including geological and structural data for deposits >0.8 t Au)
Historic mineral occurrences	>300	Predominantly minor shafts and workings
Exploration history		Detailed review of exploration history, including methods and strategies employed in previous discoveries and failures

distributions, and the spatial scales at which these systems operate. As outlined by Davies et al. (2020a), such research would also represent an important step towards modelling whole-mineral systems, in an effort to produce resource potential maps to guide exploration targeting. In addition, further studies may provide incremental improvements to the Three-part Assessment methodology, including the most appropriate composition of expert panels and elicitation processes (Davies et al. 2020b). In contrast with the currently defined endowment of 54 t gold, all grade-tonnage models utilised in this study suggest that significant gold resources remain to be discovered within the Sandstone Greenstone Belt. Given median and mean estimates of 13 for the total number of deposits, it is suggested that several additional deposits remain to be discovered, although much of the undiscovered mineral endowment will likely be defined through brownfield exploration, targeting extensions to existing ore bodies, as has been shown for the Yilgarn as a whole by Vearncombe and Phillips (2020). Based on the results of this study, it is deemed that the Sandstone greenstone belt represents an under-explored region of Western Australia, with significant orogenic gold mineralisation remaining to be discovered despite its location in the less well-endowed Youanmi Terrane.

The business of exploration: implications

The majority of the 920 km^2 Sandstone Greenstone Belt is held by two publicly listed companies (as at end-2019): Alto Metals Limited and Middle Island Resources Limited. Alto Metals holds mineral tenure for approximately 70% of the total ground and 35% of known in-ground gold resources, and Middle Island Resources approximately 15% of the ground and 60% of resources (Davies et al. 2019a: Table 6). During

Table 10. Expert workshop estimates for the number of deposits, along with summary statistics. N refers to the number of deposits corresponding to the specified confidence level, s is standard deviation of the number of deposits, CV is the coefficient of variation for deposit number estimates and P refers to the total contained gold at each specified probability level. N05 and N01 values were not estimated, but N10 values were used in their place in the calculation of CV and s. Although the experts were briefed several times that estimates for deposit numbers must align with the selected grade-tonnage model, if was deemed that the estimated deposit numbers would not materially differ between each of the three separate grade-tonnage models, given that ten deposits >0.8 t Au have already been discovered within the Sandstone Greenstone Belt.

Aggregated deposit number estimates and summary statistics						
N90	N50	N10	s	CV	$N_{(known)}$	$N_{(mean)}$
11	13	17	3.4	0.260	10	13

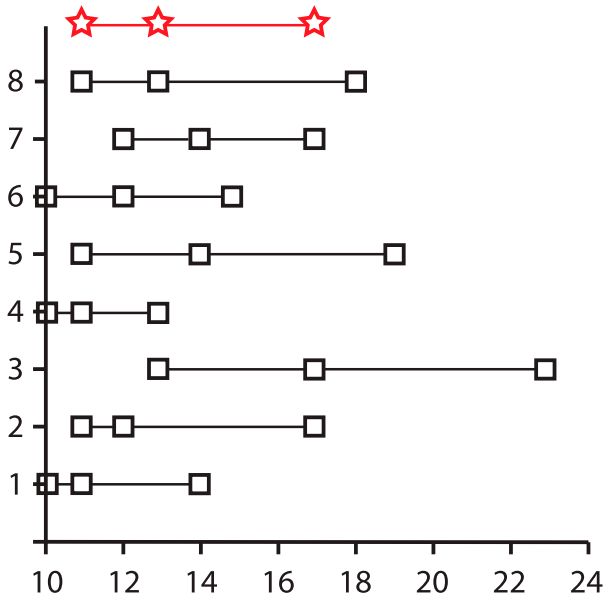

Figure 12. Individual and aggregated expert estimates for the number of orogenic gold deposits in the Sandstone Greenstone Belt. The aggregated estimates are represented by the red line with star shaped markers. The black line and square sharped markers represent individual estimates. Each marker along a single line represents the N90, N50 and N10 estimates.

2016–2019, Alto Metals released JORC 2012-compliant inferred resource estimates for the Lord Henry, Lord Nelson, Vanguard, Indomitable, Havilah and Ladybird deposits, bringing their total in-ground gold resources to >8 t (Alto Metals Limited 2019). During the same period, Middle Island Resources released a resource, albeit only inferred, totalling >10 t Au for the Two Mile Hill tonalite deeps (Middle Island Limited 2016), and continue to explore the viability of mine development (Middle Island Limited Resources 2018; Middle Island Resources Limited 2020). In 2019,

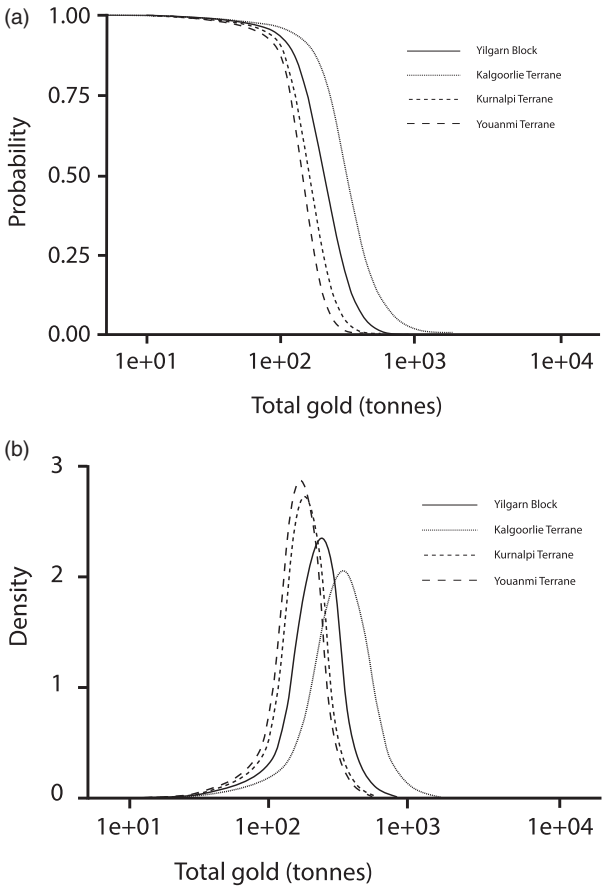

Figure 13. (A) Results of Monte Carlo simulations for the orogenic gold endowment of the Sandstone Greenstone Belt, presented as probabilistic distributions for each of the Yilgarn Block, Kalgoorlie Terrane, Kurnalpi Terrane, and Youanmi Terrane grade-tonnage models, respectively. (B) Results of Monte Carlo simulations for the orogenic gold endowment of the Sandstone Greenstone Belt, presented as density distributions for each of the Yilgarn Block, Kalgoorlie Terrane, Kurnalpi Terrane, and Youanmi Terrane grade-tonnage models, respectively.

Table 11. Summary results of Monte Carlo simulations for the orogenic gold endowment of the Sandstone Greenstone Belt. Expert workshop estimates for the number of deposits are combined with the Yilgarn Block, Youanmi Terrane, Kalgoorlie Terrane, and Kurnalpi Terrane grade-tonnage models, respectively. For the Monte Carlo simulation, the 'MARK3' modelling option (Root et al. 1992; Bawiec and Spanski 2012; Duval 2012) of MAPMARK4 was selected with a truncated normal distribution type (Ellefson 2017).

	Probability of at least the indicated amount of gold endowment (t)					Probability of at least the indicated amount of ore (Mt)				
Model	P90	P50	P10	Mean	Probability of mean or greater	P90	P50	P10	Mean	Probability of mean or greater
Yilgarn Block	121 (4.26 Moz)	219 (7.73 Moz)	340 (11.99 Moz)	225 (7.94 Moz)	47.0%	39	104	260	138	34.4%
Youanmi Terrane	100 (3.53 Moz)	166 (5.86 Moz)	241 (8.50 Moz)	167 (5.89 Moz)	49.1%	26	55	146	80	36.2%
Kalgoorlie Terrane	152 (5.36 Moz)	298 (10.51 Moz)	510 (17.99 Moz)	319 (11.25 Moz)	43.6%	47	135	378	194	32.0%
Kurnalpi Terrane	105 (3.70 Moz)	179 (6.31 Moz)	265 (9.35 Moz)	181 (6.38 Moz)	48.3%	38	94	224	119	35.4

Middle Island attempted to acquire Alto Metals in an effort to consolidate their landholdings in the belt (Middle Island Resources Limited 2019). Subsequent takeover proposals for Alto Metals from Goldsea Australia Mining Proprietary Limited (Goldsea Australia Mining Proprietary 2020) and Habrok Proprietary Limited have also been lodged (Alto Metals Limited 2020). With land access, infrastructure and a processing facility in place, these two companies continue to proactively raise funding from the market to support their continuing exploration efforts. In alignment with the results of this USGS Three-part Undiscovered Mineral Resource Assessment, the conduct of all companies reflects the view that significant undiscovered gold mineralisation, likely to support economic mining operations, remains to be discovered in the Sandstone Greenstone Belt.

Acknowledgements

This research was funded by an Australian Government Research Training Program (RTP) Scholarship and Society of Economic Geologists (SEG) Graduate Student Fellowship Grant. Thanks are due to Rebecca Seal for her continuing feedback and support. The support of this project by Alto Metals Ltd., and particularly Dermot Ryan, Mike Kammerman, and Changshun Jia, is also gratefully acknowledged.

Disclosure statement

No potential conflict of interest was reported by the author (s).

Funding

This work was supported by the Department of Education Employment and Workplace Relations Australian Government [22056287]; Society of Economic Geologists Foundation [GSF_18-05].

ORCID

Rhys S. Davies http://orcid.org/0000-0002-7645-9710
John P. Sykes http://orcid.org/0000-0001-9735-497X

References

Alto Metals Limited. 2019. Alto increases total mineral resource estimates to 290,000 oz for the Sandstone gold project. Australian Securities Exchange (ASX) Announcement.

Alto Metals Limited. 2020. Intention to make a takeover bid in respect of the ordinary shares in Alto Metals Limited. Australian Securities Exchange (ASX) Announcement.

Bawiec WJ, Spanski GT. 2012. Quick-start guide for version 3.0 of EMINERS-Economic Mineral Resource Simulator. US Geological Survey, Open-File Report 2009-1057:26.

Blewett R, Czarnota K. 2007. The Y1–P763 Project final report November 2005. Module 3-terrane structure: tectonostratigraphic architecture and uplift history of the Eastern Yilgarn Craton. Geoscience Australia record 2007/15.

Bliss JD. 1986. Grade and tonnage model of low-sulphide Au-quartz veins. In: Cox DP, Singer DA, editors. Mineral deposit models. Virginia: US Geological Survey; Bulletin 1693: p. 239–243.

Cassidy KF. 2006. Geological evolution of the eastern Yilgarn craton (EYC) and terrane, domain and fault system nomenclature. Geosci Aust Record. 5:1–28.

Cawood PA, Hawkesworth CJ. 2015. Temporal relations between mineral deposits and global tectonic cycles. Geol Soc. 393(1):9–21.

Chen SF. 2003. Atley, WA Sheet 2741. Geological Survey of Western Australia 1:100 000 Geological Series.

Chen SF. 2005. Geology of the Atley, Rays Rocks, and southern Sandstone 1:100 000 sheets. Geological Survey of Western Australia, 1:100 000 Geological Series Explanatory Notes: 42.

Chen SF, Morris PA, Pirajno F. 2006. Komatiites in the Sandstone greenstone belt, north-central Yilgarn Craton, in: GSWA 2006 extended abstracts: promoting the prospectivity of Western Australia. Geol Surv Western Aust Record. 3:20–21.

Davies RS, Groves DI, Standing JG, Trench A, Dentith M, Sykes JP. 2019a. Litho-structural controls on orogenic gold deposits within the Sandstone greenstone belt, Yilgarn Craton. Western Australia: implications for exploration targeting. Appl Earth Sci. 128(4):136–145.

Davies RS, Groves DI, Trench A, Dentith M. 2020a. Towards producing mineral resource-potential maps within a mineral systems framework, with emphasis on Australian orogenic gold systems. Ore Geol Rev. 119:103369. https://www.sciencedirect.com/science/article/pii/S0169136819308571.

Davies RS, Groves DI, Trench A, Dentith M, Sykes JP. 2019b. Appraisal of the USGS Three-Part Mineral Resource Assessment through estimation of the orogenic gold endowment of the Sandstone Greenstone Belt, Yilgarn Craton, Western Australia: Mineral Deposita, 1–20.

Davies RS, Groves DI, Trench A, Sykes JP, Standing JG. 2018. Entering an immature exploration search space: Assessment of the potential orogenic gold endowment of the Sandstone Greenstone Belt, Yilgarn Craton, by application of Zipf's law and comparison with the adjacent Agnew Goldfield. Ore Geol Rev. 94:326–350.

Davies RS, Ryan D, Groves DI, Trench A, Sykes JP, Standing JG, Jia C, Robertson W. 2017. Sandstone Goldfield. In: Phillips GN, editor. Australian Ore deposits. Melbourne: The Australasian Institute of Mining and Metallurgy; p. 279–282.

Davies RS, Trench A, Groves DI, Dentith M, Davies MJ, Sykes JP. 2020b. Assessing the variability of expert estimates in the USGS Three-part Mineral Resource Assessment Methodology: a call for increased skill diversity and scenario-based training. Ore Energy Res Geol. 2–3:100006. https://www.sciencedirect.com/journal/ore-and-energy-resource-geology/vol/2/suppl/C.

Dentith M, Mudge ST. 2014. Geophysics for the mineral exploration Geoscientist. Cambridge: Cambridge University Press. 1249p.

DMIRS. 2018. MINEDEX mines and mineral deposits database. Department of Mines, Industry Regulation and Safety.

Drew LJ, Menzie WD. 1993. Is there a metric for mineral deposit occurrence probabilities? Nonrenew Resour. 2:92–105.

Duval JS. 2012. Economic mineral resource Simulator. US Geological Survey. Open-File Report. 1344:2004–1344. https://pubs.usgs.gov/of/2009/1057/.

Ellefsen KJ. 2019. Effect of size-biased sampling on resource predictions from the three-part method for quantitative mineral resource assessment—A case study of the gold mines in the Timmins-Kirkland Lake area of the Abitibi greenstone belt, Canada (No. 2018-5149). Virginia: US Geological Survey.

Ellefson KJ. 2017. User's guide for MapMark4—A R package for the probability calculations in three-part mineral resource assessments. US Geol Surv. 7(14):1–23.

Gedest C, Zidek JV. 1986. Combining probability distributions: a critique and annotated bibliography. Stat Sci. 1:114–148.

Goldfarb RJ, Baker T, Dubé D, Groves DI, Hart CJR, Gosselin P. 2005. Distribution, character, and genesis of gold deposits in metamorphic terranes. In: Hedenquist JW, Thompson JFH, Goldfarb RG, Richards JP, editors. Economic geology 100th Anniversary volume. Littleton, CO: Society of Economic Geologists; p. 407–450.

Goldfarb RJ, Groves DI. 2015. Orogenic gold: common or evolving fluid and metal sources through time. Lithos. 233:2–26.

Goldsea Australia Mining Proprietary. 2020. Goldsea announces intention to make a cash takeover offer for Alto Metals Limited. Australian Securities Exchange (ASX) Announcement.

Groves DI. 1993. The crustal continuum model for late-Archaean lode gold deposits of the Yilgarn Block, Western Australia. Mineral Deposita. 28:366–374.

Groves DI, Goldfarb RJ, Gebre-Mariam M, Hagemann SG, Robert F. 1998. Orogenic gold deposits–a proposed classification in the context of their crustal distribution and relationship to other gold deposit types. Ore Geol Rev. 13:7–27.

Groves DI, Goldfarb RJ, Knox-Robinson CM, Ojala J, Gardoll S, Yun GY, Holyland P. 2000. Late-kinematic timing of orogenic gold deposits and significance for computer- based exploration techniques with emphasis on the Yilgarn Block, Western Australia. Ore Geol Rev. 17:1–38.

Guj P, Fallon M, McCuaig TC, Fagan R. 2011. A timeseries audit of Zipf's law as a measure of terrane endowment and maturity in mineral exploration. Econ Geol. 106:241–259.

Hagemann SG, Lisitsin VA, Huston DL. 2016. Mineral system analysis: Quo Vadis. Ore Geol Rev. 76:504–522.

Hammarstrom JM, Briskey JA, Schulz KJ, Peters SG, Bawiec WJ. 2005. Applications of a global mineral-resource assessment for addressing issues of sustainable mineral resource development. In: Barnhisel RI, Ed. 7th International Conference on Acid Rock Drainage (ICARD). American Society of Mining and Reclamation (ASMR), 3134 Montavesta Road, Lexington, KY 40502. p. 703–720.

Harjinder K, Anderson A, Shrimpton K, Harris S, Osborn M. 1999. Golden Cities – The Discovery of Gold Deposits in Archaean Granite. In: New Generation Gold Mines '99. Case Histories of Discovery. Conference Proceedings. Australian Mineral Foundation. p. 61–74.

Hronsky JMA. 2011. Self-organized critical systems and ore formation: The key to spatial targeting? Soc of Econ Geol Newsletter. 84:14–16.

Hronsky JMA, Groves DI. 2008. Science of targeting: definition, strategies, targeting and performance measurement. Aust J Earth Sci. 55(1):3–12.

Hronsky JMA, Groves DI, Loucks RR, Begg GC. 2012. A unified model for gold mineralisation in accretionary orogens and implications for regional-scale exploration targeting methods. Mineral Deposita. 47(4):339–358.

Jia C, Groves DI, Kammermann M, Ryan DM, Davies RS. 2020. Use of immobile trace-elements in gold exploration in the Neoarchean Sandstone Greenstone Belt, Yilgarn Block, Western Australia. Mineral Deposita. 55(2):241–225.

Kerrich R, Goldfarb RJ, Richards JP. 2005. Metallogenic provinces in an evolving geodynamic framework. In: Hedenquist JW, Thompson JFH, Goldfarb RG, Richards JP, editors. Economic geology 100th Anniversary volume. Littleton, CO: Society of Economic Geologists; p. 1097–1136.

Krapez B, Barley ME. 2008. Late Archaean synorogenic basins of the Eastern Goldfields Superterrane, Yilgarn Craton, Western Australia. Part III. Signatures of tectonic escape in an arc-continent collision zone. Precambrian Res. 161:183–199.

Kreuzer OP, Etheridge MA, Guj P, McMahon ME, Holden DJ. 2008. Linking mineral deposit models to quantitative risk analysis and decision-making in exploration. Econ Geol. 103:829–850.

Lisitsin VA, Dhnaram C, Donchak P, Greenwood M. 2014. Mossman orogenic gold province in north Queensland, Australia: regional metallogenic controls and undiscovered gold endowment. Mineral Deposita. 49:313–333.

Lisitsin VA, Moore DH, Olshina A, Willman CE. 2010. Undiscovered orogenic gold endowment in Northern Victoria, Australia. Ore Geol Rev. 38:251–269.

Lowe K, Ross AF. 2007. Troy resources NL. Sandstone project, Mid-West region Western Australia. Perth: Geological Survey of Western Australia.

Maddocks R, Otterman D, Doyle P. 2009. Troy resources NL. Sandstone project, Mid- West Region Western Australia. Perth: Geological Survey of Western Australia.

McCuaig TC, Beresford S, Hronsky J. 2010. Translating the mineral systems approach into an effective exploration targeting system. Ore Geol Rev. 38:128–138.

McCuaig TC, Hronsky JMA. 2014. The mineral system Concept: the key to exploration targeting. SEG 2014: Build Explor Capability 21st Century. 18:153–175.

Meyer MA, Booker JM. 2001. Eliciting and analysing expert judgement: a practical guide. Philadelphia, PA: The American Statistical Association and the Society for Industrial and Applied Mathematics. 459p.

Middle Island Limited. 2016. Updated mineral resource estimate for the Shillington & Two Mile Hill open pit deposits, Sandstone gold project, WA. Australian Securities Exchange (ASX) Announcement.

Middle Island Limited. 2018. Ore sorting trials and resource definition diamond drilling at Sandstone gold project, WA. Australian Securities Exchange (ASX) Announcement.

Middle Island Limited. 2019. Middle Island Announces a takeover Offer for Alto Metals Limited. Australian Securities Exchange (ASX) Announcement.

Middle Island Limited. 2020. 500,000oz two mile Hill deeps mineral resource at Sandstone gold project, WA. Australian Securities Exchange (ASX) Announcement.

Mole DR, Fiorentini ML, Cassidy KF, Kirkland CL, Thebaud N, McCuaig TC, Miller J. 2013. Crustal evolution, intracratonic architecture and the metallogeny of an Archaean craton. Geol Soc London, Special Publication 393, SP393-8. doi:10.1144/SP393.8

O'Hagan A, Buck CA, Daneshkhah A, Eiser JR, Garthwaite PH, Jenkinson DJ, Oakley JE, Rakow T. 2006. Uncertain judgements: eliciting experts' probabilities. Chichester: Wiley. 338p.

Rasilainen K, Eilu P, Halkoaho T, Heino T, Huovinen I, Iljina M, Juopperi H, Karinen T, Kärkkäinen N, Karvinen A, et al. 2016. Assessment of undiscovered metal resources in Finland. Ore Geol Rev. 86:896–923.

Reddy SM, Evans DAD. 2009. Palaeoproterozoic supercontinents and global evolution. Correlations from core to atmosphere. Geol Soc London Specl Publicat 323:1–26.

Riganti A, Farrell TR, Ellis MJ, Irimies F, Strickland CD, Martin SK, Wallace DJ. 2015. 125 years of legacy data at the Geological Survey of Western Australia: Capture and delivery. Geo Res J. 6:175–194.

Root DH, Menzie WD, Scott WA. 1992. Computer Monte Carlo simulation in quantitative mineral resource assessment. Nonrenew Resour. 1:125–138.

Shapiro JL. 2018. User's guide for MapMark4GUI—A graphical user interface for the MapMark4 R package. US Geol Surv. 7(18):1–19.

Singer DA. 1975. Mineral resource models and the Alaskan mineral resource assessment program. In: Vogely WA, editor. Mineral materials modeling: a state-of-the art review. Vogely, WA: Johns Hopkins University Press; p. 370–382.

Singer DA. 1993. Basic concepts in the Three-part Quantitative Assessments of undiscovered mineral resources. US Geological Survey, California, USA.

Singer DA, Menzie WD. 2010. Quantitative mineral resource assessments: an integrated approach. New York: Oxford University Press. 232p.

Van Kranendonk MJ, Ivanic TJ, Wingate MTD, Kirkland CL, Wyche S. 2013. Long-lived, autochthonous development of the Archean Murchison Domain, and implications for Yilgarn Craton tectonics. Precambrian Res. 229:49–92.

Vearncombe JR, Phillips GN. 2020. The importance of brownfields gold exploration. Mineral Deposita. 55(2):189–196.

Vielreicher N, Groves DI, McNaughton NJ, Fletcher I. 2015. The timing of gold mineralisation across the eastern Yilgarn craton using U–Pb geochronology of hydrothermal phosphate minerals. Mineral Deposita. 50:391–428.

Woodall R. 1994. Empiricism and concept in successful mineral exploration. Aust J Earth Sci. 41:1–10.

Zhang R, Pian H, Santosh M, Zhang S. 2015. The history and economics of gold mining in China. Ore Geol Rev. 65:718–727.